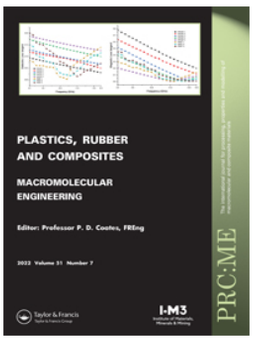

Taylor & Francis
Taylor & Francis Group

Plastics, Rubber and Composites
Macromolecular Engineering

ISSN: (Print) (Online) Journal homepage: https://www.tandfonline.com/loi/yprc20

Polymer/carbon pin through thickness reinforcement

William Moses, Thomas Dooher, Alistair McIlhagger & Edward Archer

To cite this article: William Moses, Thomas Dooher, Alistair McIlhagger & Edward Archer (2022): Polymer/carbon pin through thickness reinforcement, Plastics, Rubber and Composites, DOI: 10.1080/14658011.2022.2108981

To link to this article: https://doi.org/10.1080/14658011.2022.2108981

Published online: 08 Aug 2022.

PLASTICS, RUBBER AND COMPOSITES
https://doi.org/10.1080/14658011.2022.2108981

I·M3 Institute of Materials, Minerals & Mining
Taylor & Francis Taylor & Francis Group

Polymer/carbon pin through thickness reinforcement

William Moses, Thomas Dooher, Alistair McIlhagger and Edward Archer

School of Engineering, Faculty of Computing, Engineering & The Built Environment, Newtownabbey, UK

ABSTRACT

This work discusses the development and refinement of a polymer/fibre through thickness reinforcement method. Similar in initial concept to the traditional metalworking process of riveting this allows the manufacture of through thickness reinforced 2-D preforms. Pins are placed with deliberate excess length using a veterinary needle to part in-plane fibres. A lay-up with an array of pins is then subjected to a hot-press process flattening the pin ends resulting in a consolidated preform. This preform exhibits useful characteristics such as the ability to be cut and reformed to a new topology, with the through thickness reinforcement also conforming to the new shape. Refinements to the process introduce a multi-stage press process aimed at improving pin orientation with both original and refined processes evaluated using ASTM D5528 to determine the effect on interlaminar fracture toughness.

ARTICLE HISTORY
Received 14 March 2022
Revised 15 June 2022
Accepted 16 June 2022

KEYWORDS
Composites; through thickness reinforcement; interlaminar fracture toughness

Introduction

The issue of delamination in composite materials, and the reinforcement through the thickness of materials to resist such damage has been the subject of great study. As well as the well-established methods of Z-pinning [1–3], tufting [4–6], stitching [7–9] and 3-D weaving [10–12] authors have also attempted novel methods of achieving the goals of through thickness reinforcement [13–15].

While each method presents its own unique advantages and disadvantages. It is not uncommon to note a reduction in the in-plane properties. This is most often attributed to; the displacement of in-plane fibres around the Z direction reinforcement known as waviness in the X/Y directions and crimp in the Z direction, the damage of in-plane fibres as a result of the reinforcement process, or simply a reduction in the volume of fibre dedicated towards in-plane performance [16–19].

Materials + methods

Pinning + pressing process

The pinning process uses a commercially available 3-D printing filament manufactured by Markforged. This filament consists of a continuous fibre reinforcement encased in a Nylon matrix. In this study, two materials are evaluated – one containing carbon as the reinforcing fibre and the second containing Kevlar.

The 2-D fibre layups are constructed using a combination of Tenax 5HS-6K-375GSM satin weave carbon fibre with an areal weight of 375 g/m^2 referred to as '5HS' and Saertex ST2B Biax N Crimp 0–90 non-crimp fabric consisting of UD layers bound in a 0–90 orientation with an areal weight of 317 g/m^2 referred to as 'NCF'.

The 2-D lay-up is placed into a metal frame and clamped in place. The pinning process uses an 18 Birmingham Gauge veterinary needle. This needle is used to part the fibres allowing the easy threading of the filament through the needle. This follows a five-step process with the following list corresponding to the steps shown in Figure 1:

(a) The filament is threaded through the needle.
(b) The needle is pushed through the fabric.
(c) The filament is threaded through the needle until it hits the backstop.
(d) The needle is withdrawn while the filament is held in position.
(e) The filament is trimmed to the desired height above the surface.

This process is conducted to place an array of pins. In this study, this is conducted entirely by hand with the use of the 5HS weave pattern as a placement guide for the pins resulting in ~5 mm pin separation.

Once the desired array of pins has been placed the part may then be subjected to the press process. Initially, this press process utilised a single-stage operation. The resin transfer moulding (RTM) tool is used

CONTACT William Moses Moses-W@ulster.ac.uk

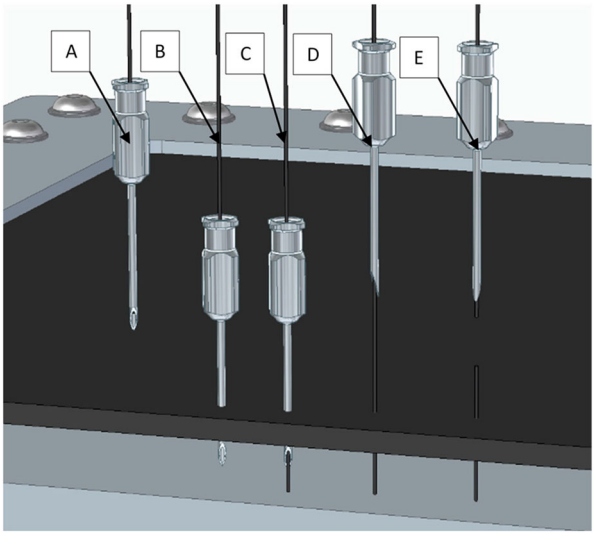

Figure 1. Representation of pinning stages.

as a convenient thermal mass heated to 150°C in an oven. The pinned fabric stack is removed from the pinning frame and placed into the tool. The lid of the tool is then bolted into place. During this time, the heat of the tool causes the pins to flatten and deform as shown in Figure 2. The tool is then left to cool to ambient temperature. While it is possible to immediately conduct infusion of the part at this point, in this study, the RTM tool was always opened for inspection of the part prior to infusion.

All sample configurations are infused using the RTM process with the resin system comprising of Gurit Prime-27 resin and Prime slow hardener this resin system offers low temperature cure and ease of mixing/infusion.

Preform characteristics

The final result of this process is a consolidated preform with 'cardboard-like' qualities. The flattened pins hold the layers together allowing ease of handling. This may be subsequently pressed a second time in a contoured tool with the pins conforming to the new geometry as shown in Figure 3.

Refinement of methods

The single-stage process presented thus far proved to have issues when evaluated in mode 1 using the ASTM D5528 [21] double cantilever beam test. The initial samples using a 12-layer 5HS lay-up with 0–90 stacking sequence demonstrated a stick-slip propagation and the shallow pin angle resulted in sub-optimal mode 1 performance. In a collaborative work with Edinburgh University [20], samples for lap-shear tests were constructed. The short overlap of the pinned region necessitated a change in the methods used. Instead of removing the part from the clamping frame used to hold the fibres in place during

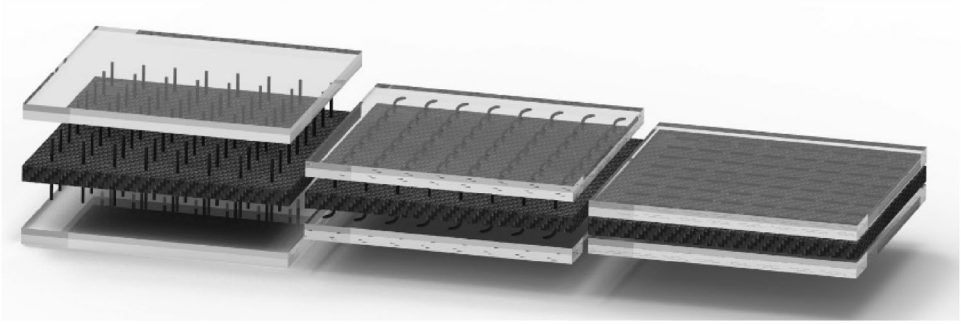

Figure 2. Illustration of the single-step process.

Figure 3. Images of re-pressed preform using an omega shaped tool.

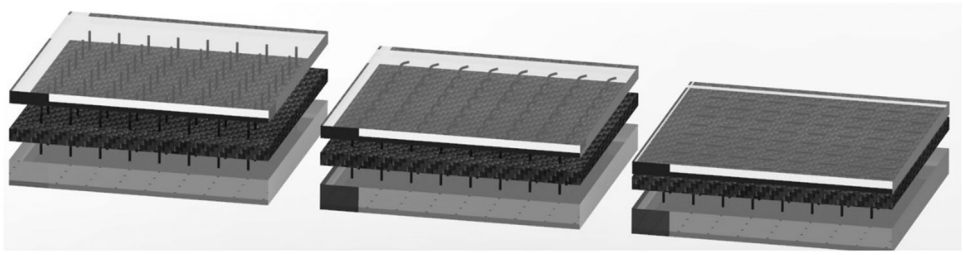

Figure 4. Stage 1 of refined press process.

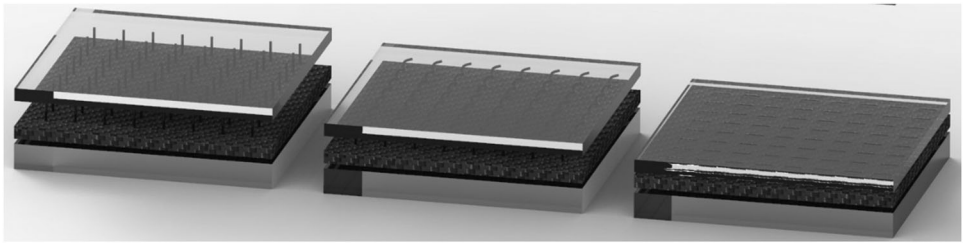

Figure 5. Stage 2 of refined press process.

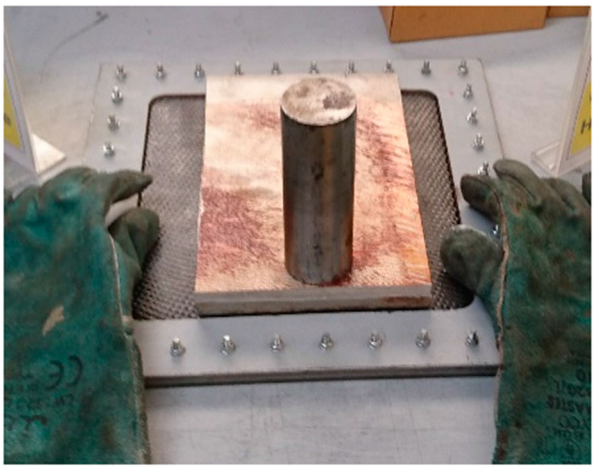

Figure 6. Example of part undergoing stage 1 press.

pinning, the part remains clamped and the pin ends are pressed in-situ. This is done with the use of a heated plate placed upon the upper layer of pins. As illustrated in Figure 4, the same backstop (lower plate of image) used during the pinning process to set consistent pass-through length is used to prevent the pins from being pushed through the fibre by the plate.

With the upper side of the pins flattened, the frame is then inverted, and the process repeated. This second press requires the sample to be supported directly below the fibre to prevent the flattened pin ends from being pushed through the part. This process is illustrated in Figures 5 and 6.

With both sides flattened the part can then be subjected to the same single-step process using the RTM

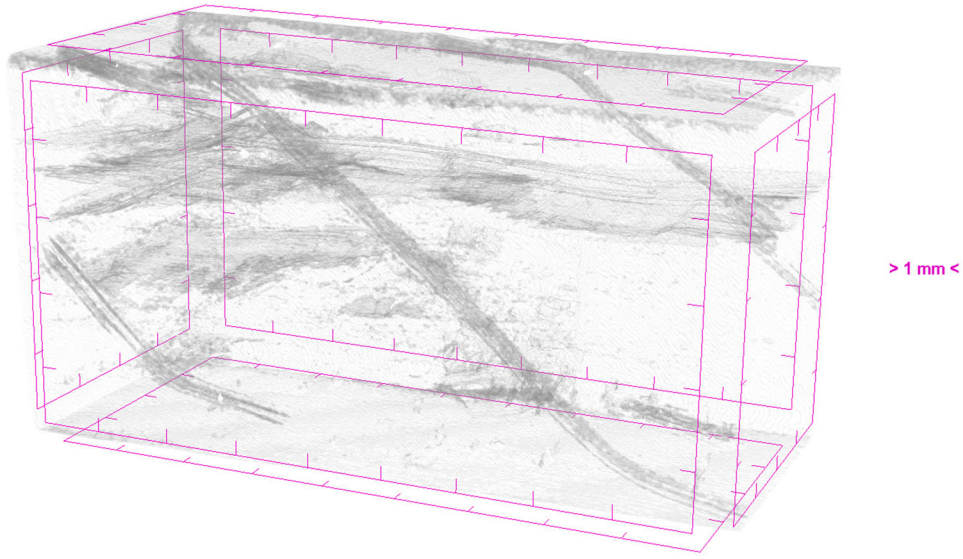

Figure 7. µCT image of pin progression from the single-stage process.

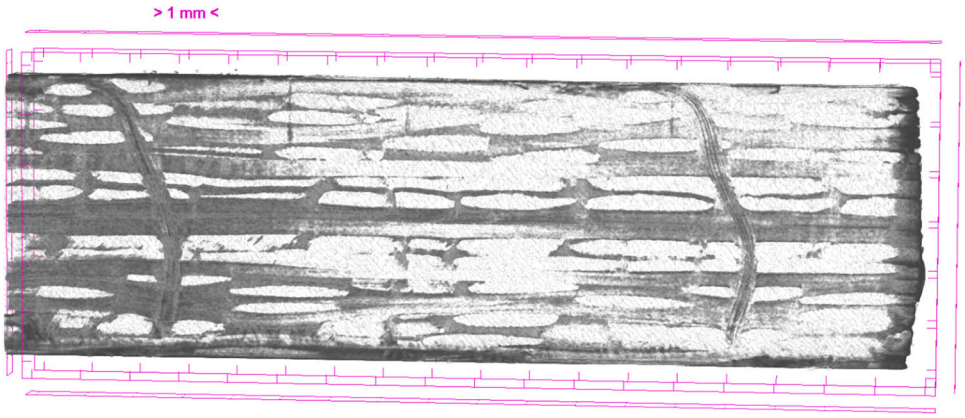

Figure 8. µCT image of pin progression in the multi-stage process.

Figure 9. Mode 1 machine + camera setup.

tool to compress the part to the final thickness for infusion.

The aim of this process is to prevent the sliding of the layers that results in a shallow pin progression in the single-stage process. µCT analysis of the single-stage process (Figure 7) shows the extent of this issue.

The refined multi-press process shows improvement (Figure 8). The pin progresses at a significantly steeper angle through the part. However, there is some level of bending in the pin. The cause of this is the compression of the part during the final press. This press is necessary for the RTM process to compact the part to the tool thickness for infusion. As the ends of the pins are flattened, they do not shift and as such the compaction results in the bending of the pins.

Mode 1

Mode 1 samples were conducted under a modified version of ASTM D5528 [21]. Samples of 25 mm width and 125 mm length were waterjet cut from the plaque with the pre-crack approximately 70 mm from the load line. The pre-crack comprised of a folded layer of Richmond Aerovac ETFE film with the fold present at the crack tip. 25 mm hinges were bonded to the part using Araldite 2014–2012 adhesive and constant crosshead displacement loading of 3 mm min^{-1} was applied by an Instron 5500R with a 5kN load cell and wedge grips. The sample hinge is mounted in the upper grip with load and then zeroed

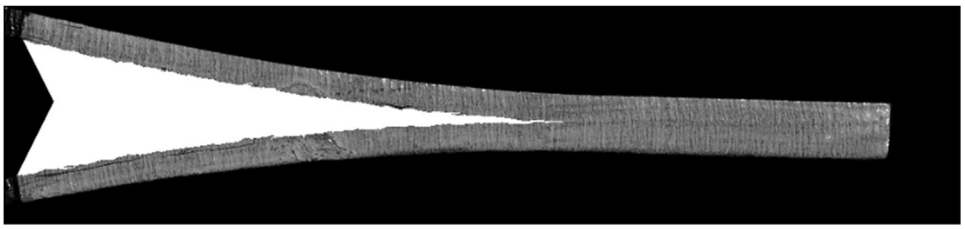

Figure 10. Example of image processing output in white overlaid on original image.

Table 1. 2-D sample configurations.

Configuration name	Test	Material lay-up	Press process
Mode 1 (Initial)	ASTM D5528M	12 layers of 5HS with repeated 0–90 lay-up samples are mirrored about the mid-plane with 0° parallel to warp.	Single stage
Mode 1 (Refined)	ASTM D5528M	10 layers of 5HS and NCF with half-sequence of: 5HS 0, 5HS 90, 5HS 0, NCF 90, NCF 0. Samples are mirrored about the mid-plane	Multi-stage

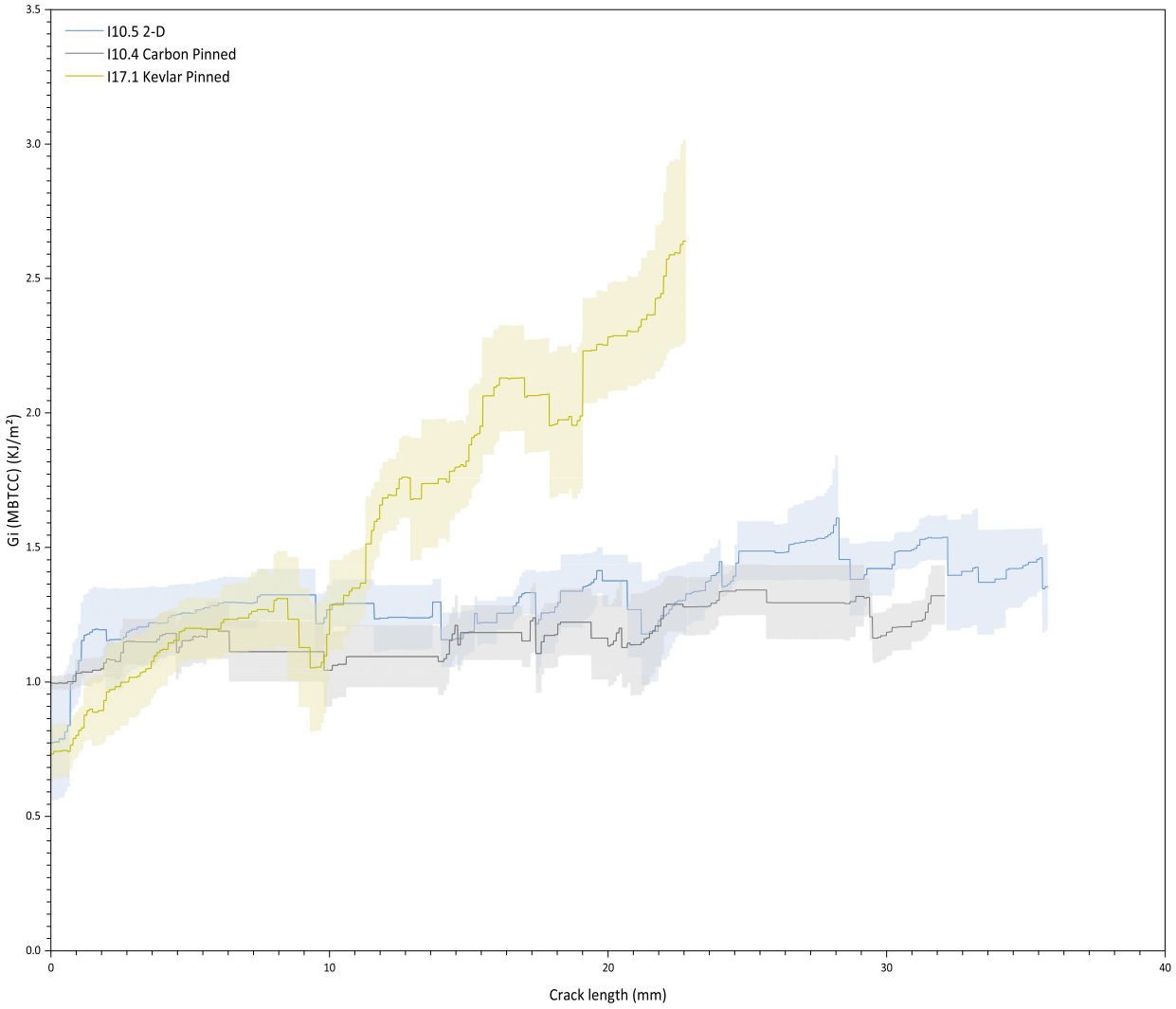

Figure 11. Mean R-curves for initial mode 1 samples. Shaded areas denote standard error over five samples.

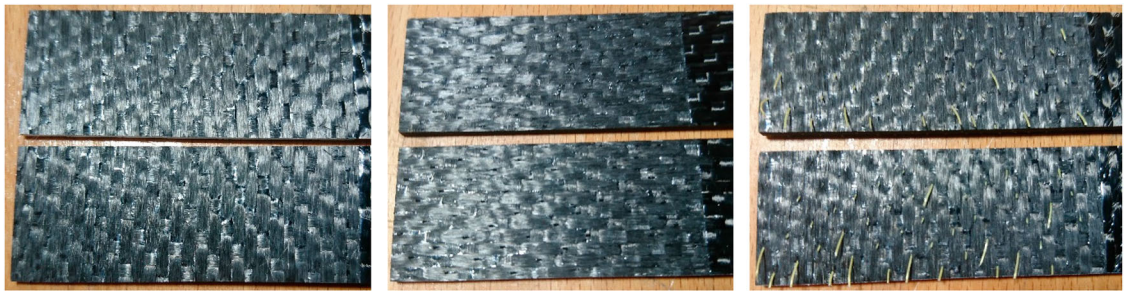

Figure 12. Images of mode 1 samples post-test. Left-right: 2-D, carbon pinned, Kevlar pinned.

to account for sample weight. The lower hinge is then mounted in the sample grip and the system manually jogged to zero load and in this position, the displacement is zeroed before test start.

The test recorded using a Y3m high-speed camera (Figure 9) samples were marked at the end of the pre-crack with measurements beyond this point recorded digitally. The camera and Instron both record data points at a rate of 4 Hz. Data synchronisation between the intron load and camera image sequence is achieved by manually correlating the final image frame to the final recorded load before failure as an easily identifiable point from both data sources.

Post-test the images are processed to provide a representation of the interior profile of the crack (Figure 10). This profile is then analysed using a C# code to provide a side-length measurement in pixels corresponding to the length of the crack. A calibration measurement using the part thickness converts this into a measurement in mm.

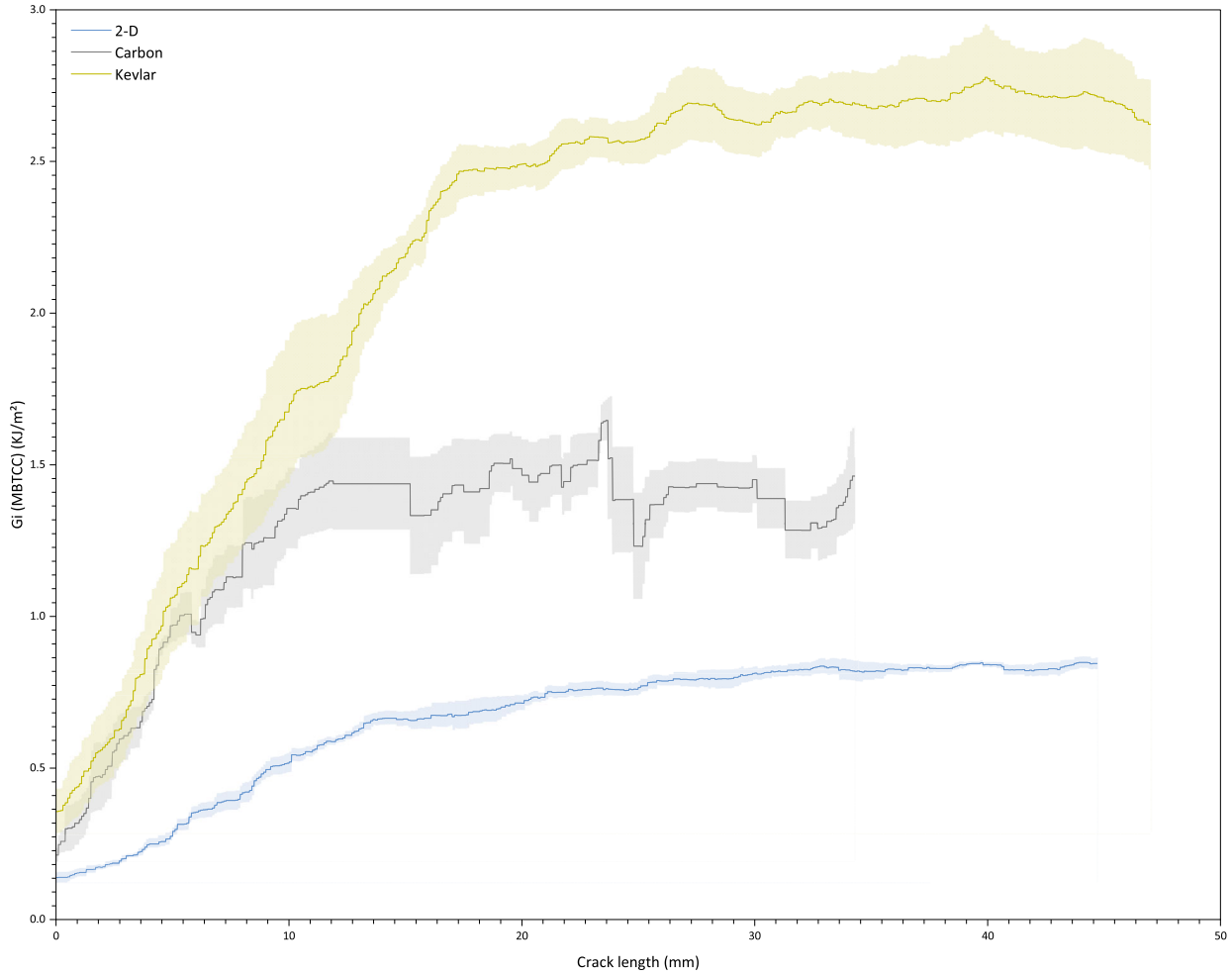

Figure 13. Mean R-curves for refined mode 1 samples. Shaded areas denote standard error over five samples.

Figure 14. Bridging observed with Kevlar samples.

From initial trials samples it was found of the various methods of analytical adjustments to Modified Beam Theory (MBT) offered under ASTM D5528 [21], the Compliance Calibration (CC) method provided the most conservative values for G_I hence all samples in this study use the MBT + CC method.

Results

Initial samples

Initial samples suffered from a high degree of stick-slip propagation as a result of the lay-up featuring woven fabric at the crack interface layer (Table 1). As can be seen in Figure 12 there is a large degree of variation in these samples resulting from this stick-slip behaviour.

Figure 11 shows the initial samples post-test. The carbon pinned samples exhibited pin fracture despite showing no notable improvement in mode 1 resistance. This is due to the shallow pin angle inducing bending/shear in the pins rather than tensile failure at the crack plane.

The Kevlar samples exhibited some degree of pull-out on the sample edges. Part of the reason for this is the angle of the pins was oriented perpendicular to the crack progression. As such pins near the edge of the part were only partially embedded allowing pull-out. However, some pins even in the centre of the part were also pulled out, indicating the pin fracture occurs near the surface of the part where the pin bends to conform to the surface.

Refined samples

The refined press method, combined with a change of lay-up to feature a UD interface, shows notable improvement. Samples with no pins (2-D), carbon pins and Kevlar pins are compared in Figure 13.

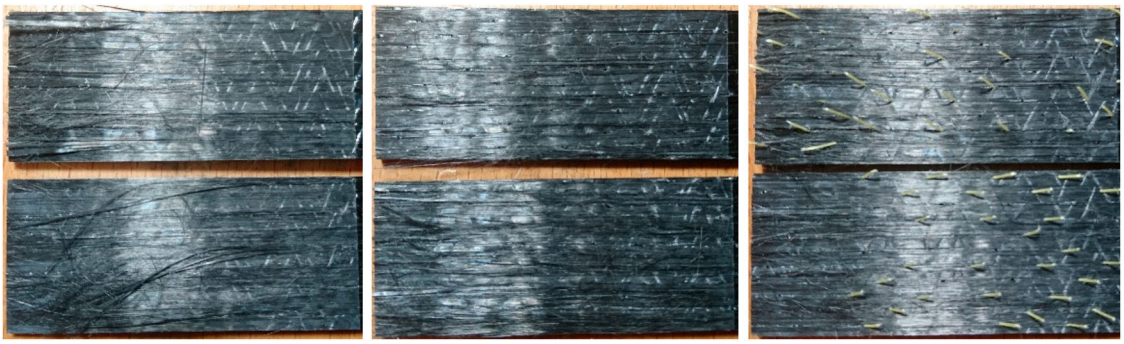

Figure 15. Images of refined samples post-test. Left-right: 2-D, carbon pinned, Kevlar pinned.

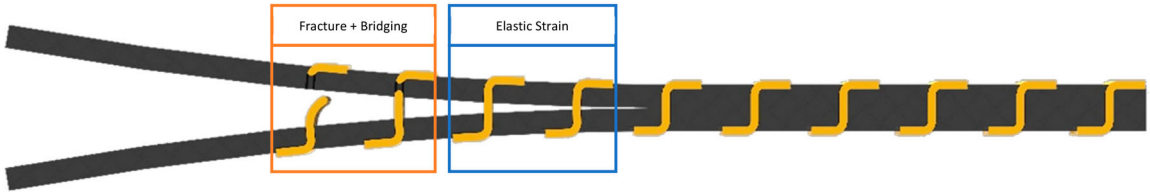

Figure 16. Illustration of fracture + bridging in Kevlar samples.

The 2-D samples exhibited smooth delamination, however the carbon pinned samples retained the stick-slip propagation. This is the result of the crack being arrested by a row of pins, with the sudden release of energy at pin fracture resulting in a corresponding increase in crack propagation. The Kevlar samples however did not experience this same phenomenon and instead exhibited the same smooth behaviour of the 2-D samples. It was observed during testing that the Kevlar pins exhibited some level of bridging (Figure 14).

Figure 15 shows images of samples post-test. The carbon pinned samples showed fracture of the pins near, although not directly on, the crack plane.

The Kevlar pinned samples however showed a high degree of pull out. observation of the top side of the part reveals that the flattened portion of the pin above the part was not disturbed indicating fracture occurs below the surface as illustrated in Figure 16. This is suspected as a cause of the smoother delamination observed as multi-pin support and frictional pull-out serve to absorb the energy release of individual pin fractures.

Conclusions

This pinning process shows promise as an alternate method of through-thickness reinforcement. The dry preform can be easily stored, handled, and manipulated into new topology while allowing the reinforcement to also conform to the new shape.

Figure 17 shows the average mode 1 results for both sample configurations. The initiation values, in this case, cannot provide meaningful conclusions, as the crack tip to first pin row separation could not be accurately controlled with the manufacturing methods used in this study.

For propagation the initial single-stage samples were hampered by the use of woven fibre, this resulted in higher values for the unreinforced composite combined with a larger degree of variation. In the case of the carbon samples, it appears that the initial samples with shallow angle are not providing meaningful support to the part with the mean within variation of the 2-D samples. When moving to the multi-stage process the carbon pinned samples showed slightly improved toughness compared to the woven variation. For these samples, however, the strength improvement is now +86% compared to the 2-D baseline.

For the Kevlar samples, there were noteworthy improvements in both configurations. This is due to the multi-pin bridging and frictional pull-out seen during the failure. It has been noted in literature that pull-out can provide increased energy absorption compared to fracture both in the case of tufted [22] and Z-pinned [23] composites.

Table 2 shows the values for both in-plane and mode 1 response of the reinforcement process demonstrated in this work compared to common methods from literature.

Further work

In terms of further work, there are three key areas of refinement that may be applied to this process. First, is the subject of automation of the pinning process to remove the time-intensive manual

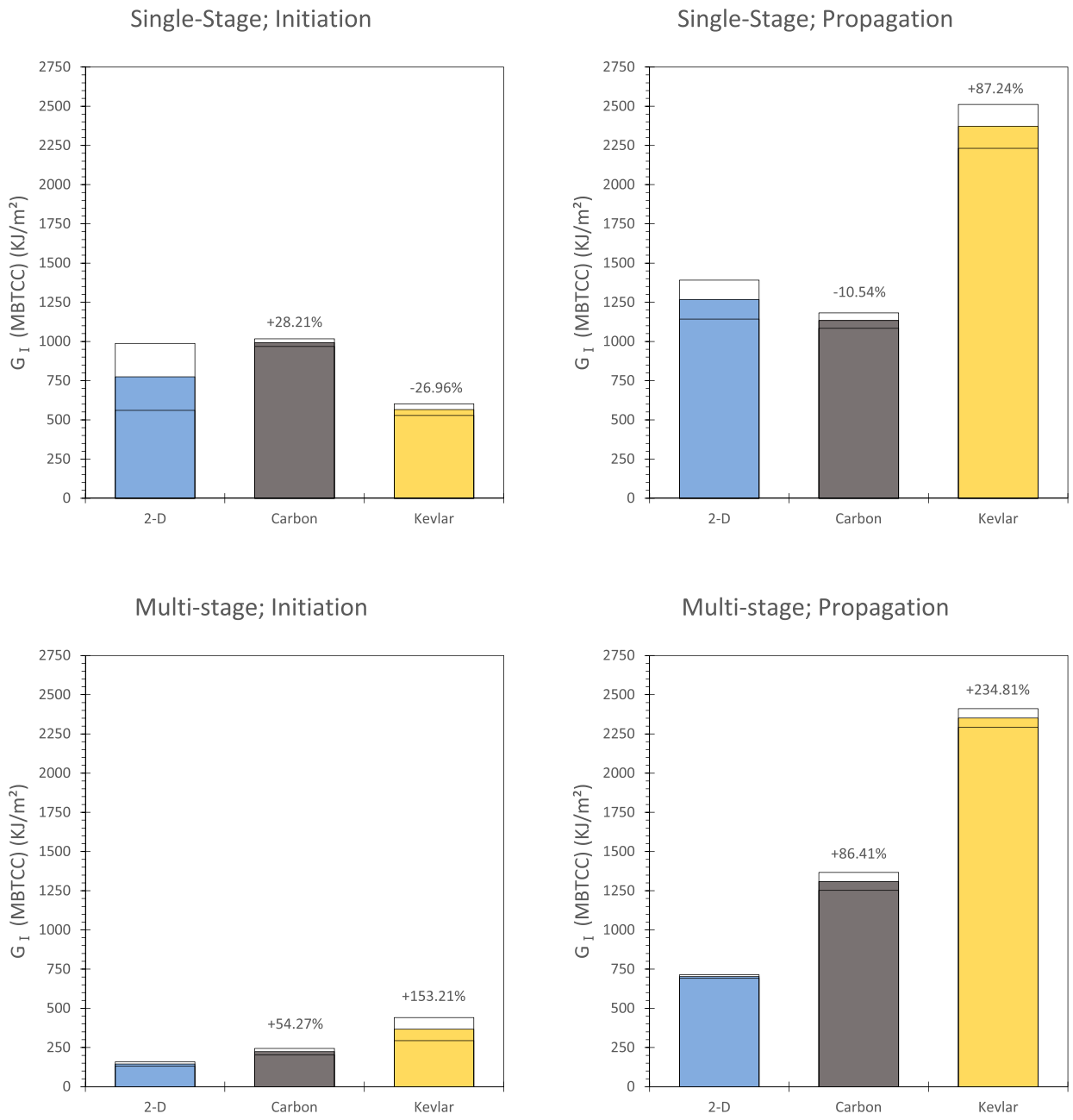

Figure 17. Charts showing initiation (left) and propagation (right) mean values for single stage (top) and multi-stage (bottom) sample configurations.

Table 2. Comparison of tensile and mode 1 properties.

Method	E	UTS	$G_{I(prop)}$
Z-Pinning [1,14,17,18,23–27]	−21% to +3.85%	−49% to +1.33%	+88% to +8439.93%
Tufting[4,5,22]	−33.84% to +8.43%	−40.61% to −10.31%	+1025%
Stitching[9,28–30]	−26.65% to +3.80%	−35.87% to +9.92%	+1.56% to +656%
Present work[a]	−11% to +2.4%	−10% to +1%	−10% to +235%

[a]Tensile values for single-stage, woven fibre sample configuration only.

process conducted in this work. Second is the investigation of further mechanical properties in particular impact resistance and mode 2/mixed mode response. Finally, is the investigation of alternate pin construction, in particular the polymer element. One candidate for this which may prove beneficial is the use of the powder epoxy investigated by Noble et al. [20]. An Epoxy based pin, if combined with a laminate constructed of the same epoxy, might allow for the construction of through thickness reinforced preforms that can act as a 'dry pre-preg' without the storage requirements associated with conventional pre-preg materials.

Disclosure statement

No potential conflict of interest was reported by the author(s).

Funding

This work was primarily sponsored by the Northern Ireland Department for the Economy (DFE) with additional support from the "Engineering and Physical Sciences Research Council", part of UK Research and Innovation (UKRI), Centre for Innovative Composites Hub (CimComp) and Spirit AeroSystems Inc (formerly Bombardier Ltd).

ORCID

William Moses http://orcid.org/0000-0002-4443-2046

References

[1] Troulis E. Effect of Z-fiber® pinning on the mechanical properties of carbon fibre/epoxy composites. Cranfield: Wharley End; 2003.
[2] Fert MM. An investigation of the mechanical performance of Z-pin reinforced composites. London, United Kingdom: Imperial College London; 2015.
[3] Dan M, Yong L, Tao S, et al. Tensile properties of Z-pins reinforced laminates. Polym Polym Compos. 2011;19(4-5):251–258.
[4] Dell'Anno G, Cartié DD, Partridge IK, et al. Exploring mechanical property balance in tufted carbon fabric/epoxy composites. Compos Part A Appl Sci Manuf. 2007;38(11):2366–2373.
[5] Bortoluzzi DB, Gomes GF, Hirayama D, et al. Development of a 3D reinforcement by tufting in carbon fiber/epoxy composites. Int J Adv Manuf Technol. 2019;100(5-8):1593–1605.
[6] Dell'Anno G, Treiber J, Partridge I. Manufacturing of composite parts reinforced through-thickness by tufting. Robot Comput Integr Manuf. 2016;37:262–272.
[7] Tan KT, Yoshimura A, Watanabe N, et al. Further investigation of delamination reduction trend for stitched composites. Compos Sci Technol. 2015;118:141–153.
[8] Dooher T, McGarrigle C, Dixon D, et al. Novel thermoplastic yarn for the through-thickness reinforcement of fibre-reinforced polymer composites. J Thermoplast Compos Mater. 2017. DOI: 10.1177/0892705717743290
[9] Mouritz A. The damage to stitched GRP laminates by underwater explosion shock loading. Compos Sci Technol. 1995;55(4):365–374.
[10] Bilisik K. Multiaxis three-dimensional weaving for composites: a review. Text Res J. 2012;82(7):725–743.
[11] Dahale M, Neale G, Lupicini R, et al. Effect of weave parameters on the mechanical properties of 3D woven glass composites. Compos Struct. 2019;223:110947.
[12] McIlhagger R, Quinn J, McIlhagger A, et al. The influence of binder tow density on the mechanical properties of spatially reinforced composites. part 2-mechanical properties. Compos Part A Appl Sci Manuf. 2008;39(2):334–341.
[13] Xu F, Huang D, Du X. Improving the delamination resistance of carbon fiber/epoxy composites by brushing and abrading of the woven fabrics. Constr Build Mater. 2018;158:257–263.
[14] Ladani RB, Ravindran AR, Wu S, et al. Multi-scale toughening of fibre composites using carbon nanofibres and z-pins. Compos Sci Technol. 2016;131:98–109.
[15] Heimbs S, Nogueira A, Hombergsmeier E, et al. Failure behaviour of composite T-joints with novel metallic arrow-pin reinforcement. Compos Struct. 2014;110:16–28.
[16] Troulis E. Effect of Z-fiber pinning on the mechanical properties of carbon fibre/epoxy composites. Cranfield, United Kingdom: Cranfield University; 2003.
[17] Hoffmann J, Scharr G. Mechanical properties of composite laminates reinforced with rectangular z-pins in monotonic and cyclic tension. Compos Part A Appl Sci Manuf. 2018;109:163–170.
[18] Knaupp M, Scharr G. Manufacturing process and performance of dry carbon fabrics reinforced with rectangular and circular z-pins. J Compos Mater. 2014;48(17):2163–2172.
[19] Mouritz AP, Cox B. A mechanistic approach to the properties of stitched laminates. Compos Part A Appl Sci Manuf. 2000;31(1):1–27.
[20] Noble T, Davidson JR, Floreani C, et al. Powder epoxy for one-shot cure, out-of-autoclave applications: lap shear strength and Z-pinning study. J Compos Sci. 2021;5(9):225.
[21] International A. ASTM D5528. Standard test method for mode I interlaminar fracture toughness of unidirectional fiber-reinforced polymer matrix composites1. West Conshohocken, PA: ASTM International; 2013.
[22] Pappas G, Joncas S, Michaud V, et al. The influence of through-thickness reinforcement geometry and pattern on delamination of fiber-reinforced composites: part I-experimental results. Compos Struct. 2018;184:924–934.
[23] M'membe B, Yasaee M, Hallett SR, et al. Effective use of metallic Z-pins for composites' through-thickness reinforcement. Compos Sci Technol. 2019;175:77–84.
[24] Knopp A, Scharr G. Tensile properties of Z-Pin reinforced laminates with circumferentially notched Z-pins. J Compos Sci. 2020;4(2):78.
[25] Loh T, Ladani R, Ravindran A, et al. Z-Pinned composites with combined delamination toughness and delamination self-repair properties. Compos Part A Appl Sci Manuf. 2021;149:106566.
[26] Mouritz A, Chang P. Tension fatigue of fibre-dominated and matrix-dominated laminates reinforced with z-pins. Int J Fatigue. 2010;32(4):650–658.
[27] Pingkarawat K, Mouritz A. Comparative study of metal and composite z-pins for delamination fracture and fatigue strengthening of composites. Eng Fract Mech. 2016;154:180–190.
[28] Pingkarawat K, Mouritz A. Stitched mendable composites: balancing healing performance against mechanical performance. Compos Struct. 2015;123:54–64.
[29] Ravandi M, Teo W, Tran L, et al. The effects of through-the-thickness stitching on the mode I interlaminar fracture toughness of flax/epoxy composite laminates. Mater Design. 2016;109:659–669.
[30] Yudhanto A, Lubineau G, Ventura IA, et al. Damage characteristics in 3D stitched composites with various stitch parameters under in-plane tension. Compos Part A Appl Sci Manuf. 2015;71:17–31.